Advanced Low-Complexity Multicarrier Schemes Using Fast-Convolution Processing and Circular Convolution Decomposition

AlaaEddin Loulou, Juha Yli-Kaakinen, and Markku Renfors, *Fellow, IEEE*

***Abstract*—Filter-bank based waveform processing has been suggested as an alternative for the plain cyclic-prefix (CP) orthogonal frequency-division multiplexing (OFDM) based schemes in fifth generation (5G) and future wireless communication systems. This is because of the new requirements, such as asynchronous and mixed numerology scenarios supporting multi-service operation in a common framework, including enhanced mobile broadband, low latency and high reliability communications, as well as low-rate machine type communications (MTC). Nevertheless, advanced multicarrier waveforms impose significantly increased computational complexity compared to the CP-OFDM scheme. Multirate fast-convolution (FC) processing has recently been proposed as an effective implementation for advanced waveforms, such as filtered OFDM (F-OFDM) and filter-bank multicarrier (FBMC) schemes, providing extreme flexibility in the subband spectral control. In this paper, we investigate the computational complexity of FC based waveform processing and propose two computationally efficient schemes using the idea of circular convolution decomposition. The first scheme targets at narrow bandwidth scenarios, such as MTC. The second scheme considers dense spectral use of non-overlapping subbands. Both schemes achieve significant reduction in the computational complexity compared to direct FC and polyphase filter-bank based implementations. This reduction in the complexity is achieved without performance loss with respect to direct FC processing. Mathematical analyses are provided for both schemes, along with evaluation and comparison of the computational complexities considering F-OFDM and FBMC waveforms in long-term evolution (LTE)-like scenarios.**

***Index Terms*—Wireless communications, 5G mobile communication, multicarrier waveforms, OFDM modulation, fast Fourier transforms, transform decomposition, fast-convolution.**

I. Introduction

THE cyclic-prefix (CP) orthogonal frequency-division multiplexing (OFDM) scheme is widely used in wireless networks due to its high flexibility in bandwidth allocation between users, simple channel equalization process using CP, and very simple and straightforward implementation using fast Fourier transform (FFT) or inverse fast Fourier transform (IFFT) [2]. The main disadvantage of CP-OFDM is its poor spectral localization. This limits the capabilities of the CP-OFDM to operate in mixed numerology and asynchronous scenarios and results in insufficient spectrum utilization due to the need of relatively wide guardbands [3]. While the spectrum utilization of long-term evolution (LTE) is about 90 %, the fifth generation new radio (5G-NR) targets at 99 %.

The next cellular mobile generation (5G) is expected to bring many new challenges to the wireless network design [4]. For instance, 5G promises gigabits per second user data rates in the enhanced mobile broadband service, as well as connecting massive number of low-rate devices through a service commonly known as massive machine type communications (mMTC). However, the current waveforms, such as CP-OFDM, are unable to cope with these new requirements.

Filter-bank multicarrier (FBMC) schemes have been widely studied as an alternative to CP-OFDM with enhanced spectral characteristics. Even though FBMC was not selected by 3rd generation partnership project (3GPP) for 5G-NR, these schemes remain as an interesting choice for future system development. FBMC schemes deliver subbands that are well localized in frequency domain using high-order filters per subcarrier. FBMC waveforms can be implemented effectively using uniform polyphase filter-banks [5]–[7]. A scheme, known as frequency spreading-FBMC (FS-FBMC) [8], is intended to emulate the polyphase-FBMC implementation using overlap-and-add (OA) processing at the transmitter and overlap-and-save (OS) processing at the receiver. This scheme introduces high flexibility in controlling the subband center frequencies and it also simplifies the channel equalization process. However, FS-FBMC has higher computational complexity than the corresponding polyphase implementations [9]. Recently, the fast-convolution filter-bank (FC-FB) scheme (also known as overlap FFT FB [10]) was proposed which can be considered as a generalization of FS-FBMC [11]. This new scheme includes an adjustable parameter for compromising between implementation complexity and degradation in signal quality, allowing significant reduction in the computational complexity with tolerable effects in the system performance. FC-FB has shown clearly reduced computational complexity per processed symbol compared to polyphase filter-banks. It also enables efficient frequency domain equalization processing [12], high flexibility in supporting non-uniform bandwidths and adjustable center frequencies, as well as mixed numerology and mixed waveform-processing capability. The scheme has proven its capability in heterogeneous wireless communication scenarios [13].

Recently, it has become obvious that 5G-NR standardization is progressing towards CP-OFDM based waveforms,

A. Loulou, J. Yli-Kaakinen, and M. Renfors are with the Laboratory of Electronics and Communications Engineering, Tampere University of Technology, FI-33101 Tampere, Finland (e-mail: alaa.loulou@tut.fi; juha.yli-kaakinen@tut.fi; markku.renfors@tut.fi).

This work was supported by the Finnish Funding Agency for Technology and Innovation (Tekes) under the Wireless for Verticals (WiVe) project. Early stage results of this paper have been published in Proc. ICC 2017, Paris, France [1].

but with novel elements enhancing their performance in the considered scenarios. Filtered OFDM (F-OFDM) scheme is a central ingredient in this development [14], [15]. Basically, this scheme consists of conventional CP-OFDM modulator and demodulator and multirate linear filtering on resource block or subband level using time-domain filters [16], [17] or polyphase filter-banks [18], [19]. F-OFDM delivers well-localized subbands compared to conventional CP-OFDM, while most of the transmission schemes and signal processing algorithms developed for CP-OFDM are directly applicable. In [20], computationally efficient technique has been proposed to reduce the complexity of universal filtered-OFDM (UF-OFDM) scheme by decomposing the time-domain processing into polyphase processing. However, this scheme does not fit into 3GPP LTE numerology, requiring some modifications to the PRB size or the sampling rate. Besides, the solution in [20] is limited to the transmitter side. Recently, the FC processing has been proposed for the filtering process of F-OFDM [21]. The use of FC-FB for F-OFDM brings a new level of flexibility in shaping the subbands in frequency domain with individually tunable subband characteristics. This scheme is referred to as FC-F-OFDM. Furthermore, it has been shown that FC-F-OFDM is computationally more efficient than the time-domain F-OFDM in most practical scenarios [22].

In this paper, we investigate the computational complexity of FC based schemes focusing on FC-FB and FC-F-OFDM. The FC processing is considered as low complexity solution for filtering sequences with long impulse responses. Nevertheless, there is possibility to further reduce the computational complexity in certain important scenarios. In [1], the authors have proposed narrowband decomposed FC-FB (NB-D-FC-FB) scheme targeting at reducing the computational complexity of narrowband transmitters. In this paper, the NB-D-FC-FB idea is extended to include the receiver side and F-OFDM waveform. Moreover, a new scheme is proposed to reduce the computational complexity in the case of uniform non-overlapping subbands scenario. The new scheme is denoted as constant-band decomposed FC-FB (CB-D-FC-FB).

Generally, in narrowband allocations it is expected that the relative complexity of transforms/filter banks grows heavily, if the transmitter or receiver processing is parametrized according to the full-band allocation. An alternative solution would be to perform the waveform processing with reduced bandwidth, corresponding to reduced transform/filter-bank size, and modify the digital and analog front-end processing structures accordingly. However, there are several reasons for considering the full-band model also when the device is operating with low data rate: (i) Fast frequency hopping and dynamic resource allocation are central elements in systems like LTE and 5G-NR and they are difficult to implement in analog way. (ii) Moving towards software-defined radio (SDR) implementations with simplified analog RF section. In this context, frequency selective waveform processing implements effectively also the needed digital channelization filtering. (iii) In any case, the devices usually need the capability to operate with full-band allocations to comply with the standards.

The main contributions of this paper can be listed as follows:

- The idea of the decomposed FC is proposed using methods similar to the transform decomposition [23], [24], also known as multi-dimensional circular convolution (CC) [25]. While the developments could be based on the Cooley-Tukey algorithm for FFT implementation [26], we use the transform decomposition approach as a more generic tool.
- The decomposition of FC is applied both on the transmitter and receiver sides.
- NB decomposition is developed for FC processing in narrowband transmitter and receiver scenarios.
- A novel and effective FC decomposition scheme is developed for scenarios with uniformly distributed non-overlapping subbands.
- Generic formulas for the complexity of the new schemes are provided and compared with direct FC-FB designs and basic reference schemes.
- The decomposed FC schemes are applied for both FBMC and F-OFDM waveforms.

Following this section, the FC based schemes are reviewed considering both FBMC and F-OFDM waveforms. Then in Section III the idea of CC decomposition is discussed and analyzed mathematically. Section IV develops the decomposition of the FC based schemes. First, the generic decomposed FC scheme is developed, followed by two efficient variants: NB-D-FC and CB-D-FC. Consequently, Section V provides the complexity analysis based on analytical expressions for the multiplication and addition rates. Section VI presents numerical results for the decomposed schemes in comparison with traditional implementations for both FBMC and F-OFDM waveforms. Finally, Section VII provides the conclusions and ideas for future work.

II. Overview of fast-convolution filter-bank

FC processing can be used for effectively implementing convolution through block-wise frequency-domain multiplications of the input data blocks with fixed filter coefficients. The multiplication in frequency-domain is equivalent to CC in time-domain, whereas the common acyclic convolution (also called linear convolution) can be obtained using either overlap-and-add (OA) or overlap-and-save (OS) type FC process. The OA process does zero padding for non-overlapping input blocks and adds up the overlapping parts of CC output blocks. The OS scheme uses partially overlapping input blocks and constructs the output from the non-overlapping parts of the CC output blocks. With sufficient overlap, both of these processes calculate the acyclic convolution precisely (limited only by the numerical precision). However, significant savings in the computational complexity can be achieved by using reduced overlap while introducing a tolerable amount of circular interference.

In this paper, we focus on the CC part of the FC processing. Therefore, the overlapping nature of the overall scheme is relevant only for the computational complexity and performance evaluation. The same FFT-domain filter coefficients are used in the direct FC-FB and proposed implementations, and the FC overlap factor λ affects in the same way in alternative realizations. Further discussions on the implementation of FC-FB and circular interference effects can be found in [11].

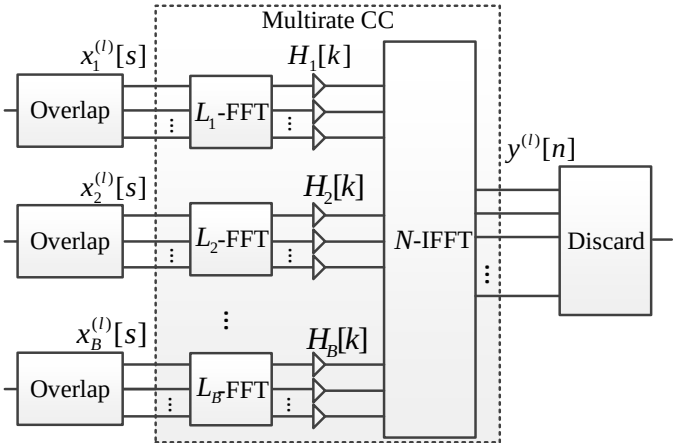

Fig. 1. The generic implementation of FC-FB based SFB using overlap-and-save processing. The dashed part of the scheme represents the multirate CC comprised in the multirate FC process.

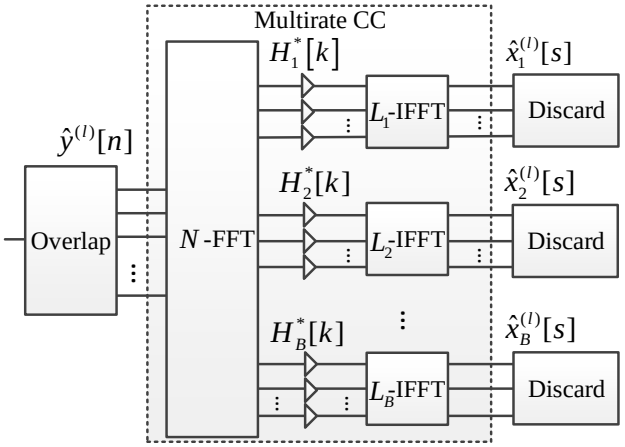

Fig. 2. The generic implementation of FC-FB based AFB using overlap-and-save processing. The dashed part of the scheme represents the multirate CC comprised in the multirate FC process.

FC based synthesis filter-bank (SFB) is shown in Fig. 1. The B low-rate incoming signals are first buffered into overlapping blocks as part of the OS block-wise process. Then, the overlapped blocks of the bth subband are fed to the input of the short (forward) transform of size L_b for $b = 1, 2, \ldots, B$. The input of the short transform is denoted as $x_b^{(l)}[s]$, where $s = 0, 1, \ldots, L_b - 1$ is the low-rate time index and l is the block index. The low-rate input $x_b^{(l)}[s]$ is the input of the multirate CC that is comprised in the multirate FC process. Here, the FC process implements multirate time-domain filtering that interpolates the input by the factor R_b with

$$R_b = \frac{N}{L_b}, \tag{1}$$

where N is the length of the long (inverse) transform [27]. The discrete Fourier transform (DFT)-domain representation of the incoming signals is obtained by the short DFT of length L_b (L_b-DFT). Each incoming signal is first modulated to the center frequency k_b by circularly shifting the DFT-domain bin values by k_b bins and then multiplying by the DFT response of the corresponding subband filter $H_b[k]$. Then, inverse discrete Fourier transforms of size N (N-IDFT) is taken from the result of the multiplication followed by discarding the overlapping samples according to OS processing. The output of N-IDFT is the output of the multirate CC with respect to $x_b^{(l)}[s]$, that is expressed as

$$y^{(l)}[n] = \frac{1}{N} \sum_{k=0}^{N-1} \sum_{b=1}^{B} H_b[k] X_b^{(l)}[\langle k - k_b \rangle_N] W_N^{-nk}, \tag{2}$$

where $n = 0, 1, \ldots, N-1$ is the high-rate time index, k is the frequency index, $\langle \cdot \rangle_N$ denotes the modulo N operation, $W_N = \exp\left[-2\pi j/N\right]$, and $X_b^{(l)}[k]$ is the L_b-DFT of $x_b^{(l)}[s]$.

Fig. 2 shows the structure of FC based analysis filter-bank (AFB). The incoming high-rate signal is first partitioned into overlapping blocks and then it is fed to the N-DFT. The input of the CC multirate process is denoted as $\hat{y}^{(l)}[n]$. Then it is multiplied by the corresponding subband filter $H_b^*[k]$. Subsequently L_b-IDFT is applied resulting in the low-rate signal $\hat{x}_b^{(l)}[s]$, which is the output of the multirate CC corresponding to the input $\hat{y}^{(l)}[n]$. Finally, the overlapping samples are discarded to obtain the FC process output. In this process, the sampling rate is reduced by the factor R_b and the output can be expressed as

$$\hat{x}_b^{(l)}[s] = \frac{1}{L_b} \sum_{k=-L_b/2}^{L_b/2-1} H_b^*[\langle k + k_b \rangle_N] \hat{Y}^{(l)}[\langle k + k_b \rangle_N] W_{L_b}^{-sk}, \tag{3}$$

where $\hat{Y}^{(l)}[k]$ is the N-DFT of $\hat{y}^{(l)}[n]$. Both (2) and (3) represent the CC multirate operation that is inherent in the FC multirate process.

A. Fast-convolution based filter-bank multicarrier waveforms

Generally, the FC-FB scheme is capable of emulating various modulation schemes, such as FBMC with offset quadrature amplitude modulation (FBMC/OQAM), filtered multitone (FMT) [28], or even single-carrier transmission with QAM/PSK modulation. The FBMC/OQAM scheme staggers (i.e., time-shifts by half symbol interval) the in-phase (I) and quadrature (Q) parts of the modulated QAM signal. This is needed to make the adjacent subcarriers orthogonal while the subcarrier spacing remains equal to that of OFDM [6]. On the other hand, the FMT scheme uses the normal (rectilinear) QAM modulation with Nyquist pulse shaping and non-overlapping subcarriers. FMT has lower spectrum efficiency than FBMC/OQAM, but it avoids certain inconvenient aspects of OQAM modulation, regarding, e.g., pilot structures for channel estimation, and it allows to utilize all multi-antenna techniques that are commonly used in OFDM systems.

In this article, the target is to simplify the evaluation of the multirate CC in FC processing. The underlying waveform processing, e.g., FBMC/OQAM or FMT, has no effect on the complexity of the proposed CC decomposition. However, different waveform schemes, in general, have different complexities which has to be taken into account when evaluating the overall complexity of the transmitter or the receiver processing. On the other hand, the proposed decomposition does not affect the performance of the waveform since the decomposed processing gives essentially the same output as

the non-decomposed one. The differences are only due to limited numerical precision.

B. Fast-convolution filtered OFDM

Basically the F-OFDM schemes apply filtering on the subband level, corresponding to single or multiple physical resource blocks (PRBs). Therefore, smaller transforms are sufficient for generating the OFDM signals for different subbands. This is followed by an upsampling and interpolating filter. The described process addresses the transmitter side. The dual operation is performed on the receiver side. The multirate filtering involved in the implementation of F-OFDM can be realized by using the polyphase-FFT structures [18], [19]. However, the configurability, that is, the possibility to adjust the channel bandwidths and center frequencies independently is very limited for these structures. Alternatively, the multirate nature of F-OFDM allows the exploitation of the FC multirate processing as proposed in [21].

In this article, our low-complexity solution tackles the CC part of the FC-F-OFDM. However, the effect of interpolation/decimation factor, bandwidth utilization, and number of subbands of this scheme affects the total computational complexity. Thus, they are considered in the complexity calculations.

III. The decomposition of circular convolution

The CC process is mathematically expressed as

$$y^{(l)}[n] = \frac{1}{N}\sum_{k=0}^{N-1} X^{(l)}[k]H[k]W_N^{-nk}, \tag{4}$$

where N is the length of DFTs and IDFT, $X^{(l)}[k]$ is the DFT of the lth input block $x^{(l)}[n]$ and $H[k]$ is the DFT of the filter impulse response $h[n]$. The process of the decomposed CC, or what is called "multi-dimensional cyclic convolution" in [25], remaps the time indexes of the input and the filter, resulting in smaller sequences. Then the CC output can be constructed from those new small sequences. Here, polyphase decomposition is applied to divide the input block and the filter impulse response in time-domain into $D = 2^m$ delay branches, where m is positive integer. Therefore, the DFTs for the decimated inputs of the delay branches and the corresponding filter responses are obtained as

$$X^{(l)}[k', d_x] = \sum_{r=0}^{\frac{N}{D}-1} x^{(l)}[rD + d_x]W_{\frac{N}{D}}^{rk'} \tag{5a}$$

$$H[k', d_h] = \sum_{r=0}^{\frac{N}{D}-1} h[rD + d_h]W_{\frac{N}{D}}^{rk'}, \tag{5b}$$

where $d_x = 0, 1, \ldots, D-1$ is the delay index of the input, $d_h = 0, 1, \ldots, D-1$ is the delay index of the filter, r is the decimated time index, and $k' = 0, 1, \ldots, N/D-1$ is used as the frequency index for reduced-size DFTs. Then the output transform is decomposed by D using the decimation-in-frequency approach. In this approach, the input is split to D parts and the output is polyphase decomposed into D delay branches. As a result, the output transform is replaced by D transforms of length N/D. The input to the decomposed output transform is expressed as

$$Y^{(l)}[k', d_y] = \sum_{d_h=0}^{D-1} X^{(l)}\left[k', \langle d_y - d_h\rangle_D\right] H\left[k', d_h\right] W_N^{aDk'}, \tag{6}$$

where $d_y = 0, 1, \ldots, D-1$ is the delay index of the output, and a is either 0 or 1. The integer a solves the sum of complex exponentials that results from the combination of the twiddle factors of the decomposed input, filter, and output. Consequently, a is defined as follows:

$$a \equiv \left\lfloor \frac{d_x + d_h}{D} \right\rfloor = \left\lceil \frac{d_h - d_y}{D} \right\rceil. \tag{7}$$

Accordingly, the resulting CC can be expressed as:

$$y^{(l)}[n] = \frac{D}{N}\sum_{k'=0}^{\frac{N}{D}-1} Y^{(l)}[k', \langle n\rangle_D]W_{\frac{N}{D}}^{-k'\lfloor \frac{n}{D}\rfloor}. \tag{8}$$

The proof is given in Appendix A.

Fig. 3(a) depicts an example of the decomposed CC when $D = 2$. The input signal is multiplexed to two sequences corresponding to the even and odd samples. Then the DFT of the delayed branches $X^{(l)}[k', d_x]$ is multiplied by the stored DFTs of the polyphase decomposed filter branches $H[k', d_h]$. The result of multiplication may be multiplied by set of twiddle factors depending on (7). Finally, the CC is obtained by upsampling and combining the delay branches of the output. Fig. 3(b) shows the CC decomposition in the case of interpolated input. In such a case, at least half of the input samples are zeros allowing to remove the second (lower) polyphase branch of the input with its corresponding operations. The CC decomposition in the case of decimated output is illustrated in Fig. 3(c), where at least half of the output samples are not needed. Therefore, the second polyphase branch of the output is not needed, allowing to discard the related operations. Figs. 3(b) and 3(c) are basic examples of employing the decomposition in multirate CC processing, which show the possibility of discarding redundant operations. This can be exploited for multirate FC in which multirate CC is the essential part of the process.

IV. Decomposition of the multirate CC

The exploitation of the CC decomposition in the FC-FB context leads to different variants of FC-FB. Some of those variants are not efficient computationally and/or degrade the flexibility in controlling the subbands bandwidths and center frequencies. First, the generic structure of the decomposed FC (D-FC) is developed and, then, its effective variants are considered in the following subsections.

A. Generic decomposition scheme

Here, the chosen decomposition factor should follow

$$D \leq R_{\min}, \tag{9}$$

where $R_{\min}$ is the smallest upsampling/downsampling factor among the subbands. This condition is needed to have only a single polyphase branch per subband as shown in Figs. 3(b)

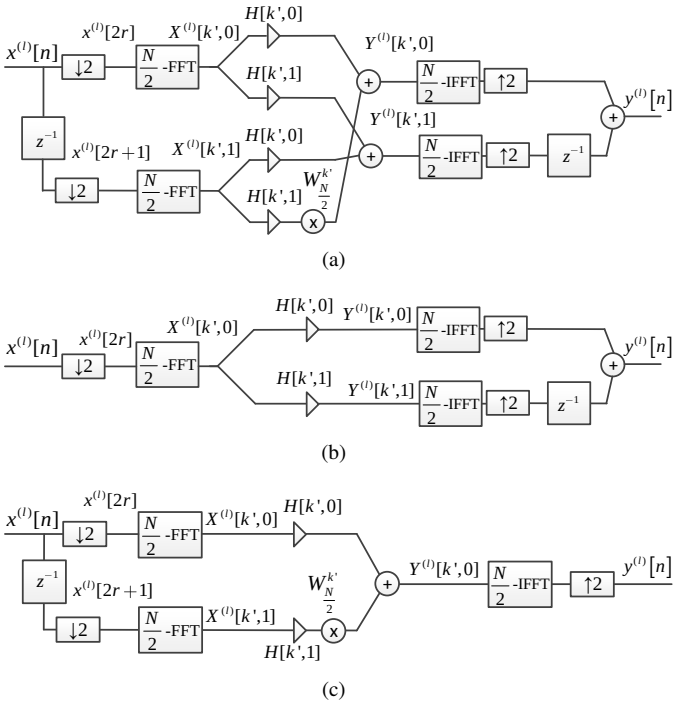

Fig. 3. The CC decomposition implementation in three cases. (a) Without multirate processing. (b) Interpolated input. (c) Decimated output.

and 3(c). This allows to discard redundant operations such as decimated transforms and filter coefficients.

Starting from the SFB side, the low-rate signal $x_b^{(l)}[s]$ is upsampled by R_b (cf. (1)). The decomposition of $x_b^{(l)}[s]$ by D results in $x_b^{(l)}[r, d_x] = 0$ for all values of d_x except when $d_x = 0$. Accordingly, the N/D-DFTs of the polyphase branches of the inputs are expressed as follows:

$$X_b^{(l)}[k', d_x] = \begin{cases} X_b^{(l)}[k'], & \text{for } d_x = 0 \\ 0, & \text{for } d_x = 1, 2, \ldots, D-1. \end{cases} \tag{10}$$

Then, the N-DFT response of the filter is generally defined as

$$H_b[k] = F_b\left[\langle k - k_b \rangle_N\right] W_N^{-\tau_b k}, \tag{11}$$

where τ_b is the delay term and $F_b[k]$ is the filter zero-phase DFT response. The zero-phase N-DFT response is defined to contain non-zero real coefficient values in the period $[\langle -L_b/2, L_b/2-1\rangle_N]$ and zeros elsewhere. For simplicity, the subbands are reindexed using their center frequencies k_b in the following analyses instead of subband indices b. Therefore, the center frequencies are mapped to

$$k_b = \Delta \frac{N}{D} + k'_b, \tag{12}$$

where Δ and k'_b are defined as

$$\Delta = \left\lfloor \frac{k_b - L_b/2}{N/D} \right\rfloor \tag{13a}$$

$$k'_b = \left\langle k_b - \frac{L_b}{2} \right\rangle_{\frac{N}{D}}, \tag{13b}$$

respectively. Thus, the DFT response of the decomposed filter can be expressed as

$$H_{k'_b,\Delta}[k', d_h] = \frac{1}{D} W_N^{-d_h k'} W_D^{-d_h(\Delta + A_{k'_b}[k'])} G_{k'_b,\Delta}[k'], \tag{14}$$

where $A_{k'_b}[k']$ is a conditional function that is defined as

$$A_{k'_b}[k'] = \begin{cases} 0, & \text{for } k' \geq k'_b \\ 1, & \text{for } k' < k'_b, \end{cases} \tag{15}$$

and $G_{k'_b,\Delta}[k']$ is the DFT response of the decomposed filter without considering the twiddle factors that result from the decomposition and it is defined as

$$G_{k'_b,\Delta}[k'] = W_N^{-\tau_{k'_b,\Delta}(k' + C_{k'_b,\Delta}[k'])} F_{k'_b,\Delta}\left[\left\langle k' + S_{k'_b,\Delta}[k']\right\rangle_N\right], \tag{16}$$

where $C_{k'_b,\Delta}[k'] = (\Delta + A_{k'_b}[k'])N/D$ and $S_{k'_b,\Delta}[k'] = -k'_b - L_{k'_b,\Delta}/2 + A_{k'_b,\Delta}[k']N/D$. In the case when the non-zero components of $H_b[k]$ are not overlapping with two sections of N/D bins, $G_{k'_b,\Delta}[k']$ is equivalent to $H_b[k]$ because $G_{k'_b,\Delta}[k'] = 0$ for $k' < k'_b$. However, if there is overlapping, $G_{k'_b,\Delta}[k'] \neq 0$ for $k' < k'_b$ due to it is circularity. Then $A_{k'_b}[k']$ adds phase shift to (14) and (16). These shifts make the components of $G_{k'_b,\Delta}[k']$ equivalent to the corresponding non-zero components of $H_b[k]$ but circularly shifted modulo N/D.

Consequently, the decimated output is acquired by substituting (10) and (14) into (6). Then, the delay indexes are expressed as follows (cf. (61)):

$$d \equiv d_y = \langle d_h \rangle_D. \tag{17}$$

Accordingly, the decimated output is expressed as

$$y^{(l)}[r, d] = \frac{D}{N} \sum_{k'=0}^{\frac{N}{D}-1} Y^{(l)}[k', d] W_{\frac{N}{D}}^{-rk'}, \tag{18}$$

where $Y^{(l)}[k', d]$ is the sum of all filtered input signals and it is defined as follows:

$$Y^{(l)}[k', d] = \frac{1}{D} W_N^{-k'd} \sum_{\substack{\Delta=0 \\ k'_b \in K}}^{D-1} Y_{k'_b,\Delta}^{(l)}[k'] W_D^{-(\Delta + A_{k'_b}[k'])d}. \tag{19}$$

Here $K \in \{0, 1, \ldots, N/D-1\}$ and $Y_{k'_b,\Delta}^{(l)}[k']$ is the product of the rotated filter $G_{k'_b,\Delta}[k']$ and the shifted DFT response of the decimated subband $X_{k'_b,\Delta}^{(l)}$, i.e.,

$$Y_{k'_b,\Delta}^{(l)}[k'] = G_{k'_b,\Delta}[k'] X_{k'_b,\Delta}^{(l)}\left[\left\langle k' - k'_b\right\rangle_{\frac{N}{D}}\right]. \tag{20}$$

By analyzing (19), it can be concluded that the sum over Δ and then the multiplication by $W_D^{-\Delta d}$ is a D-IDFT process. Because (19) is defined with respect to k', then N/D blocks of D-IDFTs are required. Furthermore, D blocks of N/D-IDFTs are required as shown in (18). The inputs of the k'th D-IDFT are originated from the frequency bins $\left[k', k'+N/D, \ldots, k'+(D-1)N/D\right]$. The twiddle factor $W_D^{-dA_{k'_b}[k']}$ is zero for $k' \geq k'_b$, meaning that the subband does not overlap with next N/D bin-section, i.e., $A_{k'_b}[k'] = 0$ for non-zero components of the masked subband. If the subband overlaps with the following N/D section, then $A_{k'_b}[k'] = 1$ for some values of k', i.e., for

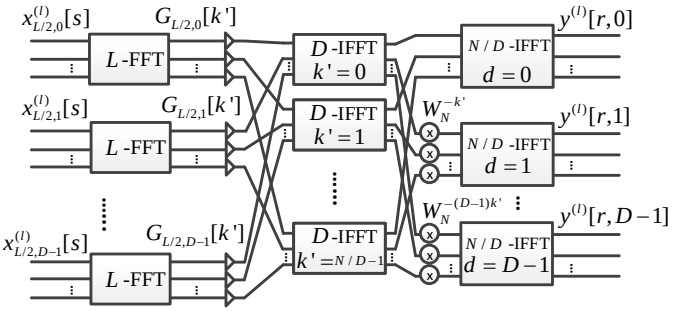

Fig. 4. The generic D-FC-SFB scheme for non-overlapping subbands of equal bandwidths $L = N/D$.

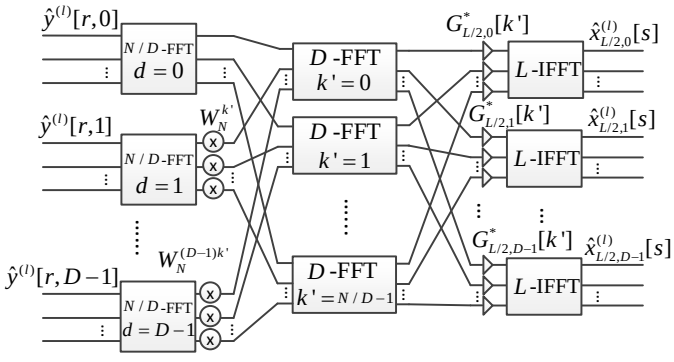

Fig. 5. The generic D-FC-AFB scheme for non-overlapping subbands of equal bandwidths $L = N/D$.

$k' < k'_b$. Accordingly, Δ is shifted by one resulting in shifting the Δth input of the k'th D-IFFT to the $(\Delta+1)$th input of the k'th D-IFFT for all overlapping frequency bins. In other words, the first stage of the D-FC-FB could be arranged in identical way as in the FC-FB. Finally, the dth output of the k'th D-IDFT is fed to the k'th input of the dth N/D-IDFT. Fig. 4 shows the implementation of the D-FC-FB based SFB. To simplify the figure, the subbands are not overlapping and they have equal bandwidths of L FFT bins.[1] However, the implementation of FC-FB using the proposed decomposition is also possible for overlapping subbands and with different bandwidths.

The analyses of the AFB are similar to the SFB case. Basically, the condition in (9) is used for restricting the choice of D. The filter on the AFB side is the complex conjugation of the filter on the SFB side, i.e., the complex conjugation of (11). Therefore, the filter is also analyzed in the same way as in (14) and (16).

In this case, the output of the AFB is decimated by R_b. Therefore, all the delay branches of the output for all values of $d_{\hat{x}}$ are zero except for $d_{\hat{x}} = 0$. As a result, it can be concluded that the delay indexes are related as follows (cf. (61)):

$$\langle -d \rangle_D \equiv d_{\hat{y}} = \langle -d_h \rangle_D. \tag{21}$$

Consequently, the decimated output of the CC is updated as

$$\hat{x}^{(l)}_{k'_b,\Delta}[s] = \frac{D}{N} \sum_{k'=0}^{\frac{N}{D}-1} \hat{X}^{(l)}_{k'_b,\Delta}\left[\left\langle k' + k'_b \right\rangle_{\frac{N}{D}}\right] W^{-k's}_{\frac{N}{D}}, \tag{22}$$

where $\hat{X}^{(l)}_{k'_b,\Delta}[k']$ is the input to the short transform and it is computed as

$$\hat{X}^{(l)}_{k'_b,\Delta}[k'] = \frac{1}{D} G^*_{k'_b,\Delta}[k'] \hat{Y}^{(l)}_{k'_b,\Delta}[k'], \tag{23}$$

where $\hat{Y}^{(l)}_{k'_b,\Delta}[k']$ is defined by the following D-DFT process:

$$\hat{Y}^{(l)}_{k'_b,\Delta}[k'] = \sum_{\substack{d=0 \\ k'_b \in K}}^{D-1} \hat{Y}^{(l)}[k',d] W_N^{dk'} W_D^{d(\Delta + A_{k'_b}[k'])}. \tag{24}$$

Accordingly, the implementation of the D-FC-AFB leads to a dual case of the D-FC-SFB as shown in Fig. 5. Therefore, the required computational complexities are expected to be the same for both SFB and AFB (while not considering the channel equalization on the receiver side). However, the number of real additions in SFB may be higher than on the AFB side if the subbands overlap in the DFT domain.

The output of the resulting scheme of D-FC-FB is identical to the corresponding FC-FB scheme (apart from effects due to finite wordlength implementation). Moreover, the long transform length is the only affected part by the decomposition. Therefore, D-FC-FB scheme does not lose any flexibility in controlling the subband center frequencies and bandwidths.

Identical result can be reached by decomposing the long transform using Cooley-Tukey algorithm for FFT implementation [26]. Similar to the idea in [23], [24], the transform should be decomposed once. Then all resulting DFTs can be implemented using split-radix FFT. Hence, the decomposition of the long transform for SFB is performed by remapping the frequency bins similar to (12) as

$$k = \Delta \frac{N}{D} + k', \tag{25}$$

where $\Delta = \lfloor Dk/N \rfloor$ and $k' = \langle k \rangle_{\frac{N}{D}}$. Consequently, the time index n is remapped as

$$n = rD + d, \tag{26}$$

where $r = \lfloor n/D \rfloor$ and $d = \langle n \rangle_D$. The output of the decomposed FC-FB is then obtained by the substitution of remapped indexes in (2). As a result, the output is expressed as

$$y^{(l)}[rD+d] = \frac{1}{N} \sum_{k'=0}^{\frac{N}{D}-1} Y^{(l)}[k',d] W^{-rk'}_{\frac{N}{D}}, \tag{27}$$

where $Y^{(l)}[k',d]$ is defined as

$$Y^{(l)}[k',d] = W_N^{-dk'} \sum_{\Delta=0}^{D-1} Y^{(l)}\left[k' + \frac{N}{D}\Delta\right] W_D^{-d\Delta}, \tag{28}$$

where $Y^{(l)}[k]$ is also defined as follows:

$$Y^{(l)}[k] = \sum_{b=1}^{B} H_b[k] X^{(l)}_b[\langle k - k_b \rangle_N]. \tag{29}$$

Accordingly, the equality between the two approaches can be tracked by comparing (27) with (18) and (28) with (19). Similarly, the Cooley-Tukey algorithm can be applied on the

[1]The same is assumed for the AFB structure of Fig. 5.

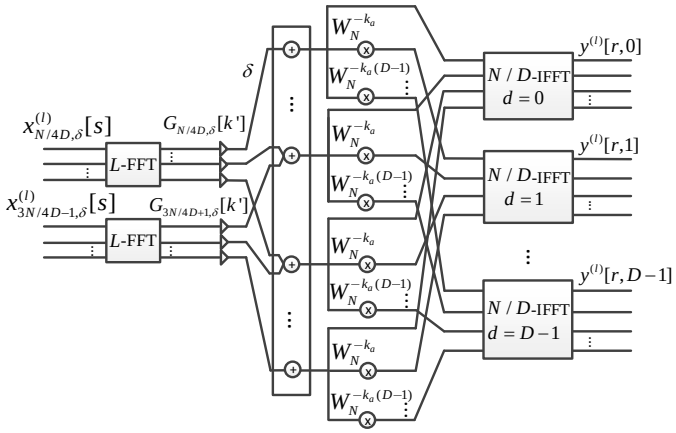

Fig. 6. NB-D-FC-FB based SFB implementation for two subbands of width $L = N/2+1$. Both subbands are contained in the δth section of the spectrum, where $k_a = k' + \frac{N}{D}\delta$.

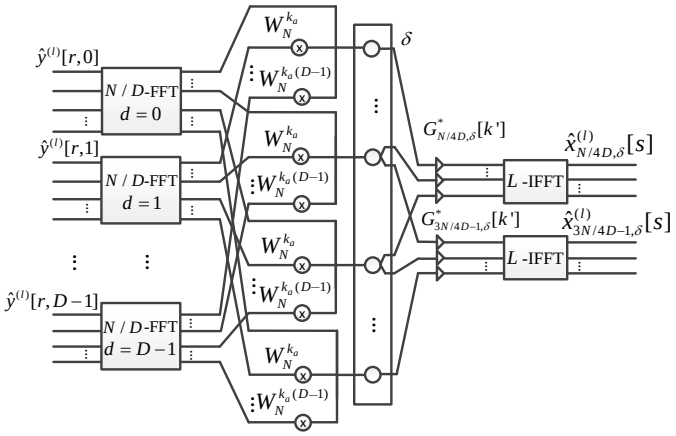

Fig. 7. NB-D-FC-FB based AFB implementation for two subbands of width $L = N/2+1$. Both subbands are contained in the δth section of the spectrum, where $k_a = k' + \frac{N}{D}\delta$.

AFB side. The resulting structure is also identical to the D-FC-FB based AFB. The equality between the two approaches holds as long as the condition (9) is valid and the DFT-domain response of the filters is zero in the period of $[L_b/2, N - L_b/2 - 1]$. Generally, the decomposition using Cooley-Tukey algorithm targets at decomposing the long transform of the FC-FB. Therefore, this approach can be used regardless of the interpolation/decimation factor R_b. On the other hand, the CC decomposition approach is more generic, meaning that it targets the whole CC part of the process. Therefore, the CC decomposition can be generalized to decompose any multirate filtering operations.

B. D-FC in narrowband scenarios

The narrowband scenario is the case when the number of active DFT bins is relatively small compared to the available ones. In such a scenario, the number of active DFT bins is small enough to prune the transforms of length D in such way that all D-IFFTs/D-FFTs have a single non-zero input/output bin at the SFB/AFB sides, respectively. Therefore, those transforms are replaced by series of twiddle factors $W_D^{-d\delta}$ and $W_D^{d\delta}$ for SFB and AFB sides, respectively, where constant $\delta \in \{0, 1, \ldots, D-1\}$ refers to the subband index with respect to the N/D sections. This leads to two stages of complex multiplications which can be replaced by single stage of multiplications by $W_N^{-d(k'+\frac{N}{D}\delta)}$ and $W_N^{d(k'+\frac{N}{D}\delta)}$ for SFB and AFB sides, respectively. The implementations of SFB and AFB type NB-D-FC-FBs are shown in Figs. 6 and 7, respectively.

The narrowband solution can be achieved if the DFT in the set $[k', k'+N/D, \ldots, k'+(D-1)N/D]$ contains a single non-zero bin. Moreover, the following condition must be satisfied

$$D \leq \frac{N}{N_k}, \tag{30}$$

where N_k is the number of active DFT bins. Any contiguous set of no more than N/D active frequency bins is applicable. Moreover, certain non-contiguous sets, following the mentioned rules, are possible. Figs. 6 and 7 show one possible contiguous set of the NB-D-FC where the used frequency bins are located in spectral section δ.

C. D-FC in constant-band scenario

Three conditions must be maintained in the subbands to be considered as constant band scenario. Firstly, the zero-phase responses of the subbands have to be equivalent. Secondly, the subbands cannot overlap in the DFT domain. Thirdly, the subbands have to be uniformly distributed, i.e., k'_b is constant for all subbands. These conditions imply that the interpolation/decimation factor R_b should be identical for all subbands. Accordingly, the short transforms have constant length of L. The constant value of k'_b implies that D must be equal to the maximum possible value $R_{\min}$. Accordingly, N/D equals:

$$\frac{N}{D} = L. \tag{31}$$

Hence, the total number of available subbands is as follows:

$$B_{\text{tot}} = D. \tag{32}$$

The subbands have constant value of k'_b as they are remapped according to Δ only. As a result, the DFT response of the decimated and delayed filter in (14) is updated as

$$H_\Delta[k', d_h] = \frac{1}{D} W_N^{-(k'+L(\Delta+A[k']))(d_h+\tau)} H[k'], \tag{33}$$

for SFB and it is expressed as

$$H_\Delta[k', d_h] = \frac{1}{D} W_N^{-(k'+L(\Delta+A[k']))(d_h-\tau)} H[k'], \tag{34}$$

for AFB, where $H[k']$ is expressed as follows:

$$H[k'] = F\left[\langle k' + S[k']\rangle_N\right]. \tag{35}$$

Here, the filter's frequency-domain weights are independent of k'_b and Δ. Therefore, the filter's weight coefficients can be combined with twiddle factors between the transforms of length N/D and the transforms of length D. Hence, the input of the N/D-IDFTs is expressed as

$$Y^{(l)}[k', d] = \frac{1}{D} W_N^{-(k'+LA[k'])(d+\tau)} H[k'] X^{(l)}[k', d], \tag{36}$$

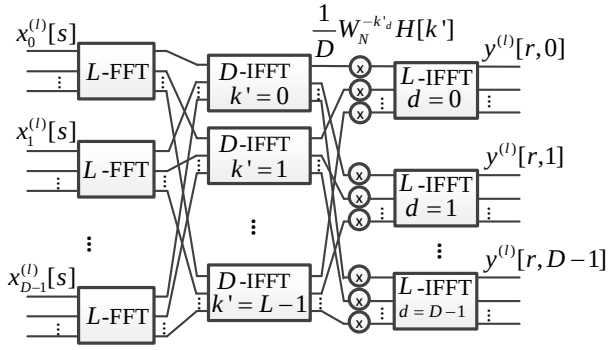

Fig. 8. CB-D-FC based SFB, where $k'_d = (k' + LA[k'])(d + \tau)$.

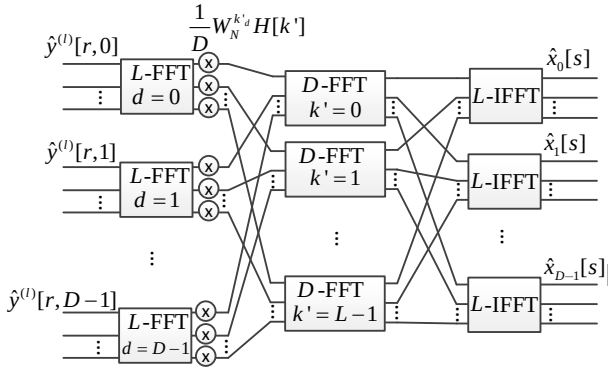

Fig. 9. CB-D-FC based AFB, where $k'_d = (k' + LA[k'])(d + \tau)$.

where $X^{(l)}[k', d]$ is expressed in the following way:

$$X^{(l)}[k', d] = \sum_{\Delta=0}^{D-1} X_\Delta^{(l)} \left[\left\langle k' - k'_b \right\rangle_{\frac{N}{D}} \right] W_D^{-\Delta(d+\tau)}. \quad (37)$$

Here, if τ is an integer, then the output of the D-IDFT can be circularly shifted by τ, i.e., $X^{(l)}[k', d + \tau]$. Fig. 8 shows the implementation of SFB based CB-D-FC. Similarly, on the AFB side, the input of the short transforms is expressed as

$$\hat{X}_\Delta^{(l)}[k'] = \frac{1}{D} \sum_{d=0}^{D-1} \hat{X}^{(l)}[k', d] W_N^{(k'+LA[k'])(d+\tau)} W_D^{\Delta(d+\tau)}, \quad (38)$$

where $\hat{X}^{(l)}[k', d]$ is defined as follows:

$$\hat{X}^{(l)}[k'] = \hat{Y}^{(l)} \left[\left\langle k' + k'_b \right\rangle_{\frac{N}{D}}, d \right] H \left[\left\langle k' + k'_b \right\rangle_{\frac{N}{D}} \right]. \quad (39)$$

In (38), the phase rotation by τ can be replaced by the circular shift at the inputs of the D-DFT if τ takes an integer value. Fig. 9 shows the implementation of the AFB based CB-D-FC.

Accordingly, the resulted CB-D-FC is similar to the generic D-FC-FB except for the combination of the filter coefficients with twiddle factors in between the transforms. Nevertheless, CB-D-FC introduces some limitations to the FC-FB structure. Firstly, the subbands cannot be overlapped limiting the applicability of this scheme. For example, CB-D-FC-FB is not applicable for FBMC/OQAM. Secondly, non-uniform subbands are not possible with this decomposed variant. Therefore, the frequency-domain equalizer weights cannot be embedded with filter weights. However, CB-D-FC-FB can be quite useful for specific scenarios, such as FMT transmitter or channelization filtering for multichannel transmitters and receivers. More specifically, the CB-D-FC can show significant reduction in the computational complexity in oversampled FMT scenarios, but not in critically sampled cases. The oversampling produces frequency replicas of the low-rate input signal. Accordingly, the number of needed D-IFFTs can be reduced by a factor equal to oversampling factor.

V. Analysis of the computational complexity

In this document, all transform lengths are assumed to be powers-of-two and the DFT and IDFT blocks are implemented using FFT and IFFT, respectively. The FFT and IFFT blocks use the split-radix algorithm which is one of the most effective algorithms for transform implementation with power-of-two lengths. The computational complexity of split-radix based transform of length N is expressed in terms of number of real multiplications and additions as

$$\mu_T[N] = N \log_2 N - 3N + 4 \quad (40a)$$

$$\alpha_T[N] = 3N \log_2 N - 3N + 4, \quad (40b)$$

respectively [29].

In the following discussions, the FC schemes are divided into four parts and the total normalized computational complexity for the FC schemes is calculated as

$$\mu = \frac{\mu^{(N)} + \mu^{(L)} + \mu_{\text{ph}}}{\eta} + \mu_{\text{OFDM}} \quad (41a)$$

$$\alpha = \frac{\alpha^{(N)} + \alpha^{(L)} + \alpha_{\text{ph}}}{\eta} + \alpha_{\text{OFDM}}, \quad (41b)$$

for real multiplications and real additions, respectively. Here, $\mu^{(N)}$ and $\mu^{(L)}$ are the number of real multiplications used to implement the long transform part and short transforms parts, respectively, and $\alpha^{(N)}$ and $\alpha^{(L)}$ are the corresponding numbers of real additions. μ_{ph} and α_{ph} are the number of real multiplications and real additions used to perform the phase rotations, when needed. In the FC-F-OFDM case, μ_{OFDM} and α_{OFDM} are the number of real multiplications and real additions needed to implemented the OFDM modulation, expressed as

$$\mu_{\text{OFDM}} = \begin{cases} \sum_{b=1}^{B} \frac{\mu_T[L_{t,b}]}{L_{u,b}}, & \text{for FC-F-OFDM} \\ 0, & \text{otherwise} \end{cases} \quad (42a)$$

$$\alpha_{\text{OFDM}} = \begin{cases} \sum_{b=1}^{B} \frac{\alpha_T[L_{t,b}]}{L_{u,b}}, & \text{for FC-F-OFDM} \\ 0, & \text{otherwise,} \end{cases} \quad (42b)$$

where $L_{t,b}$ is the length of the OFDM modulating/demodulating transform and $L_{u,b}$ is the number of active subcarriers.

The normalization factor, η, is the number of the processed QAM symbols per FC block. The input of the FC processing block can be either QAM symbols, OQAM symbols or CP-OFDM symbol multiplexes on the low-rate side. In case of FMT and FBMC/OQAM, the subchannels are two-times oversampled in the FFT-domain for Nyquist-type pulse shaping. The bandwidth is L_b FFT bins and it corresponds to two

times the symbol rate of subchannel b. With overlapping input blocks, each FC block contains $L_{s,b}/2$ QAM symbols, where $L_{s,b}$ is the non-overlapping period at the low-rate side. In FMT cases, we assume the short transform length of $L_b/2$, and oversampling is implemented in FFT-domain by copying the short transform outputs. In the FBMC/OQAM cases, the OQAM signal generation can also be done in FFT-domain, however, in a more complicated manner [30]. For simplicity, we assume L_b-length transforms in this case, since the effect in overall complexity in narrowband cases would be very small.

For FC-F-OFDM, $L_{u,b}$ QAM symbols are first modulated by $L_{t,b}$-IFFT. Then, the CP is included and the low-rate CP-OFDM symbols are processed by FC. Let $L_{\mathrm{cp},b}$ and $L_{o,b} = L_{t,b} + L_{\mathrm{cp},b}$ denote the CP-length and the total CP-OFDM symbol length, respectively, at low rate. Then the CP-OFDM symbol requires $L_{o,b}/L_{s,b}$ FC processing blocks, i.e., the number of processed QAM symbols per FC block is $L_{u,b}$ divided by the ratio $L_{o,b}/L_{s,b}$. Accordingly, the normalization factor can be calculated as

$$\eta = \begin{cases} 0.5\sum_{b=1}^{B} L_{s,b}, & \text{for FMT and FBMC/OQAM} \\ \sum_{b=1}^{B} \frac{L_{u,b}L_{s,b}}{L_{o,b}}, & \text{for CP-OFDM.} \end{cases} \tag{43}$$

Some additional computations are due to the FC-block-wise phase rotations that are required to maintain phase continuity of consecutive FC blocks [11]. This phase rotation depends on the subband center frequency and overlap factor. In specific cases, it can take trivial values, e.g., when the center frequency bin of subband b is an integer multiple of R_b or the overlapping factor is 0.5 or 0.25. Except for such special cases, the related complexities can be expressed as

$$\mu_{\mathrm{ph}} = \begin{cases} 2\sum_{b=1}^{B} L_{s,b}, & \text{for FBMC/OQAM} \\ 3\sum_{b=1}^{B} L_{s,b}, & \text{for FMT and CP-OFDM} \end{cases} \tag{44a}$$

$$\alpha_{\mathrm{ph}} = \begin{cases} 0, & \text{for FBMC/OQAM} \\ 3\sum_{b=1}^{B} L_{s,b}, & \text{for FMT and CP-OFDM,} \end{cases} \tag{44b}$$

for real multiplications and for real additions, respectively.

A. The complexity of the FC schemes

The short transforms part contains B blocks of L_b transforms and DFT-domain filtering weights. The complexity of the short transforms part is expressed as [31]

$$\mu_s^{(L)} = \sum_{b=1}^{B} \left[\mu_T \left[\frac{L_b}{\sigma} \right] + \mu_{h,b}(L_b - n_{z,b}) \right] \tag{45a}$$

$$\alpha_s^{(L)} = 2\theta + \sum_{b=1}^{B} \left[\alpha_T \left[\frac{L_b}{\sigma} \right] + \alpha_{h,b}(L_b - n_{z,b}) \right], \tag{45b}$$

where $\sigma = 2$ for the FMT cases (assuming non-oversampled low-rate signals) and $\sigma = 1$ for FBMC/OQAM and CP-OFDM cases, $n_{z,b}$ is the number of trivial weights of the filter, θ is the total number of overlapping DFT bins of two subbands with non-zero weights, and $\mu_{h,b}$ and $\alpha_{h,b}$ are coefficients that depend on filters weights as follows[2]:

$$\mu_h = \begin{cases} 3, & \text{for complex filter weights} \\ 2, & \text{for real filter weights} \end{cases} \tag{46a}$$

$$\alpha_h = \begin{cases} 3, & \text{for complex filter weights} \\ 0, & \text{for real filter weights.} \end{cases} \tag{46b}$$

These expressions are valid for both SFB and AFB sides, while not considering the equalization process on AFB side.

The other part of the FC schemes is the long transform of length N, which is considered the dominant factor in the complexity of the FC based schemes. The complexity of this part is equivalent for both the SFB and the AFB and it is computed using (40).

B. The complexity of the generic D-FC schemes

The complexity of the short transforms part in the generic D-FC scheme is equivalent to the complexity of the short transforms part in the FC schemes. Hence, the complexity expressions in (45) are applicable. Regarding the long transform part, the complexity is equivalent for SFB and AFB sides and it is calculated as

$$\mu_D^{(N)} = \sum_{d=0}^{D-1} \mu_{\mathrm{GT}}[N, D, d] + \frac{N}{D}\mu_T[D] \tag{47a}$$

$$\alpha_D^{(N)} = \sum_{d=0}^{D-1} \alpha_{\mathrm{GT}}[N, D, d] + \frac{N}{D}\alpha_T[D], \tag{47b}$$

where $\mu_{\mathrm{GT}}[N, D, d]$ and $\alpha_{\mathrm{GT}}[N, D, d]$ give the required real multiplications and real additions to implement transform of length N/D with inputs (or outputs) multiplied by $W_N^{-dk'}$ (or $W_N^{dk'}$) as defined as

$$\mu_{\mathrm{GT}}[N, D, d] = \begin{cases} \mu_T\left[\frac{N}{D}\right], & \text{for } C \in \left\{N, \frac{N}{2}, \frac{N}{4}\right\} \\ \frac{N}{D}\log_2\frac{N}{D} - \frac{N}{D}, & \text{for } C = \frac{D}{2} \\ \mu_T\left[\frac{N}{D}\right] + \beta\left[N, \frac{N}{D}, d\right], & \text{otherwise} \end{cases} \tag{48a}$$

$$\alpha_{\mathrm{GT}}[N, D, d] = \begin{cases} \alpha_T\left[\frac{N}{D}\right], & \text{for } C \in \left\{N, \frac{N}{2}, \frac{N}{4}\right\} \\ 3\frac{N}{D}\log_2\frac{N}{D} - \frac{N}{D}, & \text{for } C = \frac{D}{2} \\ \alpha_T\left[\frac{N}{D}\right] + \beta\left[N, \frac{N}{D}, d\right], & \text{otherwise,} \end{cases} \tag{48b}$$

respectively, where $C = \gcd[N, d]$ and gcd is the greatest common divisor. The $C = D/2$ case results into what is called odd-DFT [32]. The function $\beta[N, N/D, d]$ is generic complexity formula that returns the number of real multiplications and

[2]The complex multiplication requires three real multiplications and three real additions if one of the complex numbers is fixed, otherwise it costs three real multiplications and five real additions. In our case, the filter components are real numbers multiplied by twiddle factor, while the channel equalization process is not considered.

additions that are required to multiply a complex sequence by a sequence of $W_N^{k'd}$ where $k' = 0, 1, \ldots, N/D - 1$ and it is defined as follows:

$$\beta\left[N, \frac{N}{D}, d\right] = \begin{cases} 3\frac{N}{D} - \left\lceil 8\frac{C}{D} \right\rceil - 2\left\lceil 4\frac{C}{D} \right\rceil, & \text{for } \frac{N}{C} \notin \{1, 2, 4\} \\ 0, & \text{otherwise.} \end{cases} \quad (49)$$

The generic D-FC schemes require $\langle D-4 \rangle_4$ additional real multiplications with respect to FC schemes. Moreover, generic D-FC increases the number of real additions with same amount compared to FC schemes. These increases in complexity are needed on SFB and AFB sides.

C. The complexity of the NB-D-FC schemes

The complexity of short transforms part for the NB-D-FC schemes follows the formulation in (45). The number of real multiplications required to implement the long transform part is the same on the SFB and AFB sides. However, the number of additions differs because input pruning is applied on the SFB side whereas output pruning is used on the AFB side. Therefore, the number of real additions is expected to be higher on the AFB side. The complexity of the long transform part for NB-D-FC schemes is expressed as

$$\mu_{\text{NB}}^{(N)} = D\mu_T\left[\frac{N}{D}\right] + \sum_{k \in \boldsymbol{K}} \beta_P\left[N, D, k\right] \quad (50a)$$

$$\alpha_{\text{NB-s}}^{(N)} = D\alpha_T\left[\frac{N}{D}\right] + \sum_{k \in \boldsymbol{K}} \beta_P\left[N, D, k\right] \quad (50b)$$

$$\alpha_{\text{NB-a}}^{(N)} = D\alpha_T\left[\frac{N}{D}\right] + \sum_{k \in \boldsymbol{K}} \alpha_P\left[N, D, k\right], \quad (50c)$$

for real multiplications on SFB and AFB sides, real additions on SFB side, and real additions on AFB side, respectively. Here $\boldsymbol{K} \in \{0, 1, \ldots, N-1\}$ is the set of active DFT bins and $\beta_P[N, D, k]$ returns the number of real multiplications and real additions required to implement N-DFT with a single input located at index k for output in the period $[0, D-1]$ and it is expressed as

$$\beta_P[N, D, k] = \begin{cases} \frac{N}{2C} - 2, & \text{for } \frac{N}{C} \notin \boldsymbol{N_c}, \frac{N}{4C} \leq D \\ D + \frac{N}{4C} - 2, & \text{for } \frac{N}{C} \notin \boldsymbol{N_c}, \frac{N}{8C} < D < \frac{N}{4C} \\ 3D - 3, & \text{for } \frac{N}{C} \notin \boldsymbol{N_c}, D \leq \frac{N}{8C} \\ 0, & \text{otherwise,} \end{cases} \quad (51)$$

where $C = \gcd[N, k]$. This function is also valid for computing the required number of real multiplications to implement N-DFT with a single output located at index k for input in the period $[0, D-1]$. For the similar case, $\alpha_P[N, D, k]$ returns the number of real additions and it is expressed as follows:

$$\alpha_P[N, D, k] = \begin{cases} 2\frac{N}{C} + 2D - 16, & \text{for } \frac{N}{C} \notin \boldsymbol{N_c}, \frac{N}{C} \leq D \\ 4D - 2\left\lceil 8\frac{CD}{N} \right\rceil, & \text{for } \frac{N}{C} \notin \boldsymbol{N_c}, \frac{N}{4C} \leq D < \frac{N}{C} \\ 3D + \frac{N}{4C} - 4, & \text{for } \frac{N}{C} \notin \boldsymbol{N_c}, \frac{N}{8C} < D < \frac{N}{4C} \\ 5D - 5, & \text{for } \frac{N}{C} \notin \boldsymbol{N_c}, D \leq \frac{N}{8C} \\ 2D - 2, & \text{otherwise.} \end{cases} \quad (52)$$

In (51) and (52), the complexity evaluations for $D \geq N/(4C)$ are based on removing the redundant multiplications by trigonometric components [33]. In such case, the complex multiplication is implemented using four real multiplications and two real addition. This is more efficient than the three real multiplications and three real additions implementation of the complex multiplication in the case of redundancy.

The complexity of NB-D-FC scheme is dominated by three factors, N, D, and N_k. Mainly, N_k and N determine the number of the required twiddle factors and length of the transforms, respectively. Therefore, the complexity of NB-D-FC is directly proportional to both N_k and N. However, the configuration of N and N_k is not typically determined according to complexity minimization. This leaves D as the complexity design factor that can be found as

$$D_{\text{lst}} = \frac{N}{(3N_k + 4)\ln 2}, \quad (53)$$

for fixed values of N and N_k to minimize (50a). Here, we consider the common case of non-redundancy in (51) when $D \leq N/(8C)$. In this contribution, the value of D must be power of two, whereas (53) usually results in non-power-of-two value. Therefore, the actual value of D is found by direct substitution in (50a) with the next smaller and larger power-of-two value and comparing the results. Regarding allocations with very low number of active subcarriers, $N_k \leq 7$, the optimal value can be obtained directly by the maximum of (30).

Generally, the NB-D-FC scheme reduces the computational complexity by performing the FC operation by D transforms of size N/D with multiplications by twiddle factors, as shown in (50), rather than single transform of size N as in original FC based schemes. Moreover, this scheme surpasses the use of N/D transforms of size D as in generic D-FC by performing multiplication by twiddle factor. Therefore, the small number of active frequency bins implies low number of multiplications with the twiddle factors, leading to the significant reduction in the computational complexity. Nevertheless, the increase in the number of active bins may lead to insignificant complexity reduction of NB-D-FC compared to the FC based schemes or the generic D-FC.

D. The complexity of the CB-D-FC schemes

The implementation of the CB-D-FC schemes contains a small variation in its structure compared to the other FC schemes. The change is in the combination of the twiddle factors with filter coefficients. Therefore, the short transforms part of the CB-D-FC schemes contains only the short transforms and the complexity is expressed as follows:

$$\mu_c^{(L)} = B\mu_T\left[\frac{L}{\sigma}\right] \quad (54a)$$

$$\alpha_c^{(L)} = B\alpha_T\left[\frac{L}{\sigma}\right]. \quad (54b)$$

The long transform part of the CB-D-FC schemes contains L transforms of length D, D transforms of length L, and the

combination of the twiddle factors with filter's weights. The complexity of the long transform part is computed as follows:

$$\mu_c^{(N)} = D\mu_T[L] + \frac{L}{\sigma}\mu_T[D] + 3D(L-1) \tag{55a}$$

$$\alpha_c^{(N)} = D\alpha_T[L] + \frac{L}{\sigma}\alpha_T[D] + 3D(L-1). \tag{55b}$$

Given the short transforms length L and long transform length N, the CB-D-FC requires fewer real multiplications than FC scheme if B satisfies:

$$B > \frac{DL\left(\frac{1}{\sigma}-1\right)\left(\log_2 D - 3\right) + 4\frac{L}{\sigma} + D - 4}{\mu_h(L-n_z)}. \tag{56}$$

Here, n_z plays a key role in defining the CB-D-FC efficiency. In other words, the number of non-trivial filter weights specifies the effectiveness of CB-D-DC compared to the corresponding direct FC scheme.

VI. Numerical results

In this section, the computational complexity of the different decomposed schemes is evaluated and compared to the conventional FC implementation. Besides, LTE-like scenarios are considered for testing the effectiveness of the decomposed FC variants in comparison with other multicarrier schemes without considering the complexity required for the channel equalization. Therefore, the number of real multiplications needed to implement the transmitter and the receiver corresponds to equivalent functionality for all considered schemes. To obtain consistent results, the correspondence of the compared schemes is specified by the number of active subbands or subcarriers.

A. Comparisons of the decomposed schemes with conventional FC schemes

Firstly, the complexity of NB-D-FC scheme is compared with the direct FC scheme. The main factors of NB-D-FC complexity is the choice of the decomposition factor D considering the number of active frequency bins N_k and long transform length N. Here, the assumption is that N_k is fixed. This number is chosen to be three overlapping active FBMC/OQAM subcarriers of $L = 16$ FFT bins. Therefore, the subbands overlap in 8 frequency bins with adjacent subbands resulting in $N_k = 32$ active frequency bins. The long transform lengths are chosen to be 512, 1024, 2048, and 4096. Different configurations of D are shown in Table I where $D_{\max}$ is the maximum value of D according to (30), D_{lst} is the optimal value according to (53), and D_{opt} is the most efficient power-of-two value of D near to D_{lst}. Fig. 10 shows the reduction in the number of real multiplications given in percentages for NB-D-FC scheme with respect to the corresponding FC scheme. These results confirm the formulation in (53). Moreover, the reduction ratio is proportional to the ratio N/N_k. Hence, this scheme becomes more efficient when the number of active frequency bins is relatively reduced.

The second evaluation shows the significance of the CB-D-FC scheme when compared with the direct FC scheme. The main factors affecting the complexity are the decomposition factor D, the short transforms length L, the number of active subbands B, and long transform length N. Assuming fixed $L = 16$, $n_z = 2$, and $\sigma = 1$, as well as varying B, then D is configured by (31). Therefore, D equals 8, 16, 32, 64, and 128 for long transforms lengths of 128, 256, 512, 1024, and 2048, respectively. Fig. 11 shows the reduction in number of real multiplications given in percentages for CB-D-FC scheme with respect to FC scheme. These results show the increased reduction in the real multiplications with the increased number of active subbands. Moreover, it is shown that 15 % reduction in the real multiplications is expected when 87.5 %, 81.25 %, 84.3 %, 90.6 %, and 100 % of total available subbands are used for $N = 128, 256, 512, 1024$, and 2048, respectively. Moreover, the results show that the CB-D-FC scheme actually increases the computational complexity when the number of active subbands B is smaller than the limit in (56). This is indicated in Fig. 11 by the negative values for the complexity reduction for $B < 3, 3, 4, 5$, and 7 for $N = 128, 256, 512, 1024$, and 2048, respectively.

TABLE I
The Decomposition Factor Configuration of NB-D-FC Scheme for $N_k = 32$ active frequency bins.

N	N/N_k	$D_{\max}$	D_{lst}	D_{opt}
512	16	16	6.84	8
1024	32	32	13.68	16
2048	64	64	27.36	32
4096	128	128	54.72	64

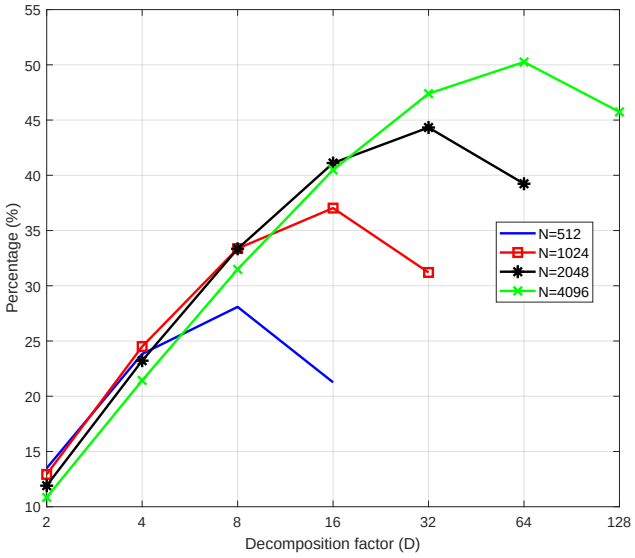

Fig. 10. The reduction in real multiplications given in percentages for NB-D-FC with respect to direct FC with $N_k = 32$ active frequency bins.

B. LTE-like scenarios

The comparison with NB-D-FC schemes is performed in 20 MHz LTE-like scenario. Here the subcarriers spacing is 15 kHz with 1200 active subcarriers out of 2048 available subcarriers. The NB-D-FC scheme is compared with direct FC based FBMC/OQAM (FC-OQAM), polyphase

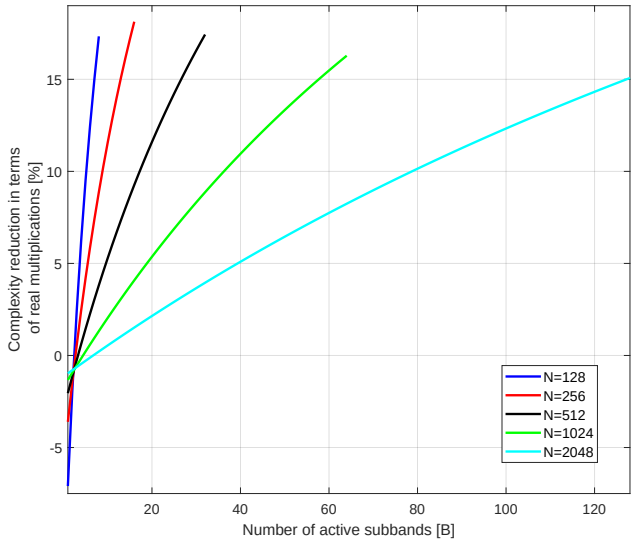

Fig. 11. The reduction in real multiplications given in percentages for CB-D-FC with respect to direct FC with $L = 16$.

FBMC/OQAM, FC-F-OFDM, and CP-OFDM as a reference scheme.[3] The standard CP length on the high-rate side is 144 samples, however, it is chosen to be 128 for FC-F-OFDM scheme.[4] This choice is made to avoid non-integer values for the CP in the low-rate side for power-of-two short transform lengths. Generally, the choice of the overlap factor $\lambda = 1 - L_{s,b}/L_b$ for FC based schemes is based on the system requirements. Small λ achieves low computational complexity with increase in the out-of-band emission and in-band interference level [28]. Even with $\lambda = 1/4$, the in-band signal-to-interference ratio is clearly above 30 dB, which is sufficient for 256-QAM modulation. With $\lambda = 1/2$, the circular distortion due to reduced overlap becomes insignificant [28]. Table II shows the parameterizations of the used schemes assuming contiguous set of active subbands. All considered schemes have 15 kHz subcarrier spacing, and have the total of 2048 available subbands.

The first test in the 20 MHz scenario compares NB-D-FC-OQAM with FC-OQAM and polyphase FBMC/OQAM. The decomposition configuration parameters of NB-D-FC-OQAM are shown in Table III. Fig. 12 shows the superiority of NB-D-FC-OQAM over FBMC/OQAM and FC-OQAM in terms of complexity. The computational complexity of the FBMC/OQAM has been found according to the complexity formulas in [36]. The NB-D-FC-OQAM reduces the required number of real multiplication by 43.5 % when compared with the corresponding FC-OQAM for single active PRB of 12 subcarriers case with $\lambda = 1/2$. With $\lambda = 1/4$, NB-D-FC almost reaches the complexity of basic CP-OFDM. In this case, NB-D-FC-OQAM reduces the number of real multiplications by 43.5 % when compared with the corresponding FC-OQAM for single active PRB.

In the second evaluation in the 20 MHz scenario, we compare NB-D-FC-F-OFDM with FC-F-OFDM. Here the configu-

[3]In narrowband scenarios, the CP-OFDM complexity could be reduced through (I)FFT pruning. Since we focus on spectrally enhanced waveforms, we do not consider reduced complexity CP-OFDM schemes here. CP-OFDM is included as a general reference, widely considered to have acceptable complexity for practical deployments.

[4]A way to reduce the short transform length of FC-F-OFDM while maintaining the compatibility with LTE and 5G-NR numerologies is presented in [34]. This approach is applicable also with the decomposed FC schemes.

TABLE II
PARAMETERIZATION OF DIFFERENT SCHEMES IN 20 MHZ LTE-LIKE SCENARIO

The scheme	Configuration
CP-OFDM	Transform length: 2048 CP length: 144
Polyphase FBMC/OQAM	Transform length: 2048 Phydyas prototype filter [8], [35] Overlapping factor: 3 and 4 No CP
FC-OQAM	Long transform length: 16384 Short transform length: 16 λ: 1/2 and 1/4 Non-trivial filter weights: 14 No CP
FC-F-OFDM	Long transform length: 2048 Short transform length: 16, 32, and 64 λ: $L/2$ and $L/4$ Non-trivial filter weights: 4 CP length: 128

TABLE III
THE DECOMPOSITION FACTOR CONFIGURATIONS FOR NB-D-FC-OQAM.

PRBs	N/N_k	$D_{\max}$	D_{lst}	D_{opt}
1	158	128	73	64
2	82	64	39	32
3	55	32	26	32
4	42	32	20	16
5	34	32	16	16

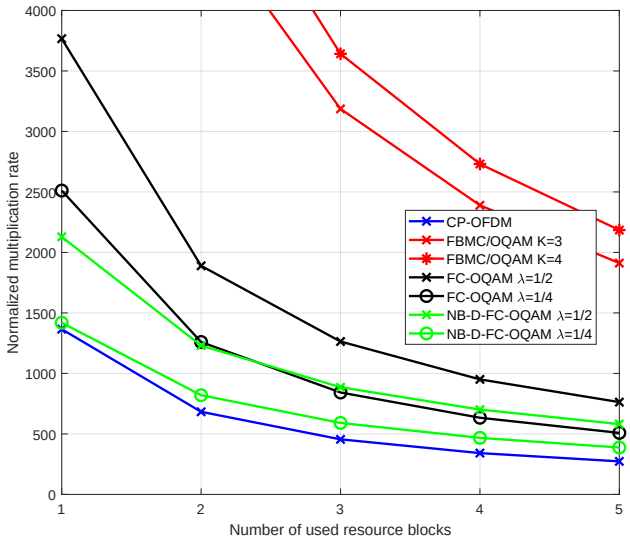

Fig. 12. The normalized number of real multiplications per QAM symbol as a function of the active bandwidth in 20 MHz scenario for FBMC/OQAM schemes with basic CP-OFDM as reference.

TABLE IV
THE DECOMPOSITION FACTOR CONFIGURATION OF THE NB-D-FC-OFDM.

PRBs	N/N_k	$D_{\max}$	D_{lst}	D_{opt}
1	128	128	49	64
2	73	64	31	32
3	51	32	22	32
4	39	32	18	16
5	32	32	14	16

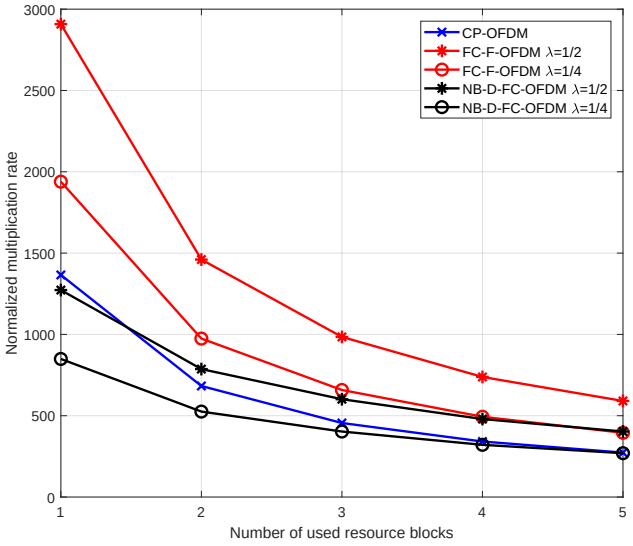

Fig. 13. The normalized number of real multiplications per QAM symbol as a function of the active bandwidth in 20 MHz scenario for F-OFDM schemes with basic CP-OFDM as reference.

ration considers the case of single subband that contains 1 to 5 PRBs, i.e., 12 to 60 subcarriers. Therefore, the short transforms lengths of the FC-F-OFDM scheme are chosen to be 16 for 1 active PRB, 32 for 2 active PRBs and 64 for 3, 4, and 5 active PRBs. The configuration of the decomposition factor for NB-D-FC-OFDM is shown in Table IV. Fig. 13 shows the superiority of NB-D-FC-OFDM with respect to other schemes in terms of complexity. For $\lambda = 1/2$, the reduction in number of real multiplications per processed QAM symbol for NB-D-FC-OFDM is 6.8 % with respect to CP-OFDM and 56.2 % with respect to corresponding FC-F-OFDM when single PRB is active. For $\lambda = 1/4$, NB-D-FC-OFDM is superior to CP-OFDM in terms of complexity. Specifically, NB-D-FC-OFDM reduces the number of real multiplications per QAM symbol by 32.3 % with respect to CP-OFDM in the case of single active PRB. Considering one alternative use case where 1-5 PRBs are filtered as individual subbands, the complexity evaluation indicates quite similar savings as above. In both Figs. 12 and 13, the reduction in the multiplication rate of the NB-D-FC schemes with respect to FC schemes is reduced when the number of PRBs is increased. Moreover, the computational complexity of the NB-D-FC becomes higher than that of direct FC-F-OFDM when the number of active PRBs exceeds 56 (out of 100) in the 20 MHz LTE scenario.

Next, CB-D-FC-FMT is compared with FC-FMT using the

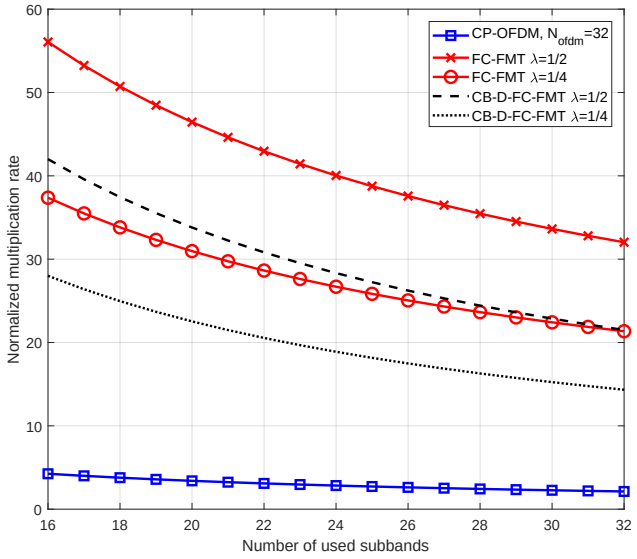

Fig. 14. The normalized number of real multiplications per QAM symbol for CB-D-FC based FMT as a function of the active bandwidth in 480 kHz bandwidth scenario.

short transform size of $L/2$ and expanding the input to double bandwidth in the FFT domain by copying the transform output, effectively realizing oversampling by two. Short transform of size of $L_b = 8$ is chosen to construct subbands of 16 FFT-bins. The results of Fig. 11 show that 15 % saving in real multiplication rate is achieved in the case of $N = 512$ and $\sigma = 1$ with more than 26 active subbands. The saving can be improved when oversampling is employed, as in the FMT scenario with $\sigma = 2$. In such cases, more than 25 % saving in the real multiplication rate is achieved when there are more than 15 active subbands. The decomposition factor in this case has to be 32 which is also equivalent to the number of available subbands. Therefore, the FMT schemes here are compared with OFDM with 32 subcarriers as reference. This represents a non-standard case of narrowband transmission with 480 kHz bandwidth assuming 15 kHz subcarrier spacing. Fig. 14 shows that CB-D-FC-FMT requires fewer real multiplications than the corresponding FC-FMT scheme. The reduction in real multiplications is from 25.1 to 32.9 % per QAM symbol.

C. Link performance aspects

As mentioned, the proposed decomposed structures for FC-FB based waveform processing produce the same output signals as the corresponding direct FC-FB implementations. The differences are only due to different round-off error accumulation models of different computational algorithms. In Matlab simulations, the worst-case differences between time-domain signals generated by direct and decomposed FC structures were about 10^{-12} times the average sample value. Analyzing the finite wordlength effects in different FC schemes remains as a topic for future studies.

Regarding the spectrum localization of transmitted signals, Fig. 15 shows an example of the FBMC/OQAM signal spectra obtained by direct and decomposed FC-FBs and polyphase FBs. We cannot see any differences between the direct and

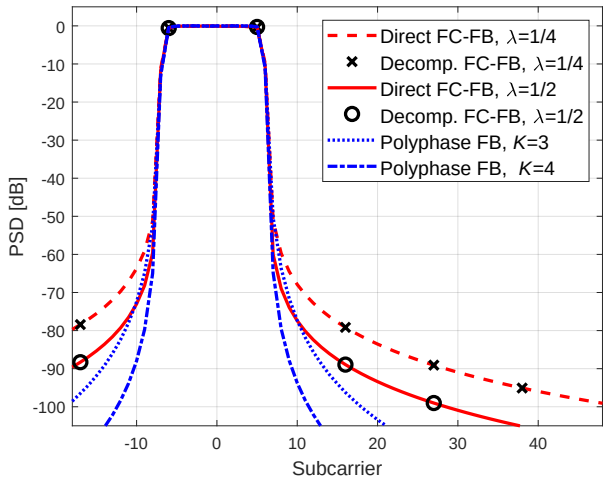

Fig. 15. PSDs for FBMC/OQAM realizations using a polyphase FB with overlap factors of $K \in \{3, 4\}$ and FC-FB with $L = 16$ and overlap factors of $\lambda \in \{1/4, 1/2\}$. The PSDs are integrated over the subcarrier spacing of 15 kHz, while using 12 active subcarriers out of 2048 in total. In both direct and decomposed FC-FB cases, the inband signal-to-interference ratio due to circular distortion is 36 dB and 44 dB with $\lambda = 1/4$ and $\lambda = 1/2$, respectively.

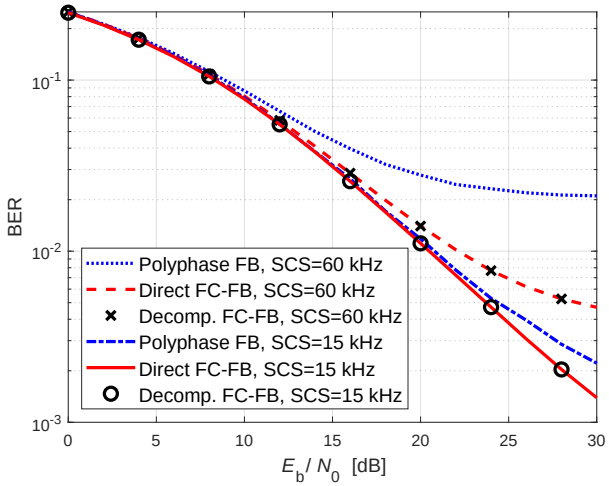

Fig. 16. Bit error-rate (BER) performance of polyphase FB ($K = 4$) and FC-FB ($\lambda = 3/8$) realizations of FBMC/OQAM in TDL-C channel with 1 µs RMS delay spread. One active PRB of 12 subcarriers with 15 kHz or 60 kHz subcarrier spacing (SCS).

decomposed FC cases. The polyphase designs apply the widely used frequency sampling based prototype filters [8], [35] with overlap factors of $K = 3$ and $K = 4$. Both polyphase and FC approaches provide very sharp transition bands. At −50 dB level, the differences in the power spectral densities (PSDs) between corresponding polyphase and fast-convolution FBs are marginal. The differences are mainly in the out-of-band emission (OBE) floor levels. Increasing the FC overlap reduces the OBE and in the extreme case with $\lambda = 1 - 1/L$, which is equivalent to the FS-FBMC scheme, the direct and decomposed FC spectra are equal to that of the corresponding polyphase filter bank. However, the computational complexity is greatly increased with increasing FC overlap. Depending on the scenario, FC overlap factors between $\lambda = 1/4$ and $\lambda = 1/2$ give sufficiently low OBE due to FC-FB imperfections. While polyphase FB with optimized prototype filters [37] reach higher stobband attenuation, the OBE characteristics are mainly determined by the spectral regrowth due to the non-linearity of the transmitter power amplifiers [38].

Link level bit error-rate (BER) comparisons between FC-FB and polyphase FB based FBMC/OQAM are shown in Fig. 16. Again, the direct and decomposed FC approaches provide identical performance. Here the tapped delay line type C (TDL-C) channel model with root-mean-square (RMS) delay spread of 1 µs and about 8.6 µs maximum delay spread is used [39]. With such relatively high delay spread, FC-FB with embedded channel equalizer provides clearly better performance than polyphase filter-bank with the typical three-tap subcarrier equalizers. The embedded equalizers can be realized without increasing the multiplication rate by combining the channel equalizer coefficients with the FFT-domain filtering weights, while the three-tap subcarrier equalizer approach for polyphase filter-bank realization slightly (by 12 real multiplications per QAM symbol) increases the multiplication rate. With high mobility, the performance of the embedded equalizer slightly degrades in the high-SNR region due to the increased processing block length [12]. As for the F-OFDM waveforms, the superior flexibility and performance-complexity tradeoff of FC-FB over alternative schemes was demonstrated in [22]. In this case, the practical way for channel equalization is to use the basic CP-OFDM equalizer model for each subband independently.

VII. Conclusion

This paper proposed the use of circular convolution decomposition for the implementation of fast-convolution based communication waveform processing. It was also indicated how equivalent decomposition can be achieved using the multidimensional convolution or Cooley-Tukey FFT algorithms.

The generic decomposed scheme has similar (slightly higher) complexity as direct FC processing and it could be useful for flexible hardware implementations supporting different system parameterizations with configurable long transform size, also with non-power-of-two values. More importantly, in specific application scenarios, appropriate decomposition schemes provide quite significant reduction in the complexity.

The NB-D-FC variant was developed for narrowband scenarios in which the number of active frequency bins is relatively small. In such scenarios, up to 50 % savings in the real multiplication rate could be achieved compared to the conventional FC. NB-D-FC was exploited in the implementation of both FBMC/OQAM and F-OFDM, with similar savings. In the case of F-OFDM with up to five active PRBs, the NB-D-FC-F-OFDM scheme was shown to require fewer multiplications per QAM symbol than the basic CP-OFDM.

Another proposed decomposition variant, namely CB-D-FC, targets at scenarios of non-overlapping identically filtered and uniformly distributed subbands. This scheme has shown up to 32.9 % reduction in the real multiplication rate. However, this scheme lacks the flexibility of the original FC-FB.

FC-FB and its decomposed variants can be used for implementing efficiently any of the existing time-domain filtering

[16], [17] or filter-bank [18], [19] based filtered OFDM schemes, by emulating in FFT-domain processing the specific time-domain filter(-bank) design. However, the FC approach allows direct design of the FFT-domain filter weights with optimized tradeoff between inband interference and OBE [22].

Our future work on decomposed FC processing is focused on applications of NB-D-FC-F-OFDM in specific important narrowband transmission scenarios, like spectrally enhanced cellular narrowband Internet-of-things (NB-IoT) and massive machine-type communications (mMTC) in the 5G new radio context. Moreover, the implementation of the FC decomposition can be extended to cover CP-OFDM scheme in narrowband scenarios.

Appendix A
Proof of the circular convolution decomposition

In this section, it is given the proof of that $y[n]$ in (4) and (8) are equivalent. Given the DFT responses of both $x^{(l)}[n]$ and $h[n]$, $X^{(l)}[k]$ and $H[k]$ are expressed with respect to (5a) and (5b), respectively, as follows:

$$X^{(l)}[k] = \sum_{d_x=0}^{D-1} X^{(l)}\left[\langle k\rangle_{\frac{N}{D}}, d_x\right] W_N^{d_x k} \tag{57a}$$

$$H[k] = \sum_{d_h=0}^{D-1} H\left[\langle k\rangle_{\frac{N}{D}}, d_h\right] W_N^{d_h k}. \tag{57b}$$

Here the decimation in time is employed. Subsequently, we define $Y^{(l)}[k, d_x, d_h] = X^{(l)}\left[\langle k\rangle_{N/D}, d_x\right] H\left[\langle k\rangle_{N/D}, d_h\right]$ for simplicity. As a result, the CC output can be expressed as

$$y^{(l)}[n] = \frac{1}{N}\sum_{k=0}^{N-1}\sum_{d_h=0}^{D-1}\sum_{d_x=0}^{D-1} Y^{(l)}[k, d_x, d_h] W_N^{(d_x+d_h-n)k}, \tag{58}$$

by substituting (57) in (4). Then, the decimation in frequency processing (it is here decimation in time because of the use of inverse transform) polyphase decomposes the output according to $n = Dr + d_y$ and divides the $Y^{(l)}[k, d_x, d_h]$ into continuous parts according to $k = k' + d_p N/D$ where d_p is the part index. Those parts are equivalent because of the periodicity of $Y^{(l)}[k, d_x, d_h]$ over N/D, i.e., $Y^{(l)}[k' + d_p N/D, d_x, d_h] = Y^{(l)}[k', d_x, d_h]$. Thus the output can be rewritten as follows:

$$y^{(l)}[Dr + d_y] = \frac{1}{N}\sum_{d_h=0}^{D-1}\sum_{d_x=0}^{D-1}\left[\sum_{d_p=0}^{D-1} W_D^{(d_x+d_h-d_y)d_p}\right] \times\left[\sum_{k'=0}^{\frac{N}{D}-1} Y^{(l)}\left[k', d_x, d_h\right] W_N^{(d_x+d_h-d_y)k'} W_{\frac{N}{D}}^{-rk'}\right]. \tag{59}$$

The sum of complex exponential over d_p is solved as

$$\sum_{d_p=0}^{D-1} W_D^{(d_x+d_h+d_y)d_p} = \begin{cases} D & \text{for } d_x + d_h - d_y = aD \\ 0, & \text{otherwise,} \end{cases} \tag{60}$$

where a is integer. Here the equality can be solved in either following ways:

$$\begin{aligned} d_h + d_x &= aD + d_y \\ \langle d_h + d_x\rangle_D &= \langle aD + d_y\rangle_D \\ \langle d_h + d_x\rangle_D &= d_y \end{aligned} \tag{61a}$$

or

$$\begin{aligned} d_y - d_h &= d_x - aD \\ \langle d_y - d_h\rangle_D &= \langle d_x - aD\rangle_D \\ \langle d_y - d_h\rangle_D &= d_x. \end{aligned} \tag{61b}$$

Accordingly, a is solved as follows:

$$\begin{aligned} \left\lfloor \frac{d_h + d_x}{D} \right\rfloor &= \left\lfloor a + \frac{d_y}{D} \right\rfloor \\ \left\lfloor \frac{d_h + d_x}{D} \right\rfloor &= a \end{aligned} \tag{62a}$$

or

$$\begin{aligned} \left\lceil \frac{d_h - d_y}{D} \right\rceil &= \left\lceil a - \frac{d_x}{D} \right\rceil \\ \left\lceil \frac{d_h - d_y}{D} \right\rceil &= a. \end{aligned} \tag{62b}$$

Consequently, we substitute (60) in (59) resulting in the following

$$y^{(l)}[Dr + d_y] = \frac{D}{N}\sum_{k'=0}^{\frac{N}{D}-1}\sum_{d_h=0}^{D-1} Y^{(l)}\left[k', \langle d_y - d_h\rangle_D, d_h\right] \times W_N^{ak'} W_{\frac{N}{D}}^{-rk'}, \tag{63}$$

where $y^{(l)}[Dr + d_y]$ is the IDFT of $Y^{(l)}[k', d_y]$ in (6). The CC output is then expressed as

$$y^{(l)}[n] = y^{(l)}\left[\left\lfloor \frac{n}{D} \right\rfloor D + \langle n\rangle_D\right], \tag{64}$$

where $r = \lfloor n/D \rfloor$ and $d_y = \langle n\rangle_D$.

References

[1] A. Loulou, J. Yli-Kaakinen, and M. Renfors, "Efficient fast-convolution based implementation of 5G waveform processing using circular convolution decomposition," in *Proc. IEEE Int. Conf. Commun. (ICC)*, Paris, France, May 22–23 2017, pp. 1–7.

[2] E. Dahlman, S. Parkvall, and J. Sköld, *4G: LTE/LTE-Advanced for Mobile Broadband*, 2nd ed. Oxford, UK: Academic Press, 2014.

[3] R. Gerzaguet *et al.*, "The 5G candidate waveform race: A comparison of complexity and performance," *EURASIP Journal on Wireless Communications and Networking*, vol. 2017, no. 1, pp. 1–13, 2017.

[4] M. Shafi *et al.*, "5G: A tutorial overview of standards, trials, challenges, deployment, and practice," *IEEE J. Select. Areas Commun.*, vol. 35, no. 6, pp. 1201–1221, Jun. 2017.

[5] M. Bellanger and J. Daguet, "TDM-FDM transmultiplexer: Digital polyphase and FFT," *IEEE Trans. Commun.*, vol. 22, no. 9, pp. 1199–1205, Sep. 1974.

[6] P. Siohan, C. Siclet, and N. Lacaille, "Analysis and design of OFDM/OQAM systems based on filterbank theory," *IEEE Trans. Signal Processing*, vol. 50, no. 5, pp. 1170–1183, May 2002.

[7] B. Farhang-Boroujeny, "OFDM versus filter bank multicarrier," *IEEE Signal Processing Mag.*, vol. 28, no. 3, pp. 92–112, May 2011.

[8] M. Bellanger, "FS-FBMC: An alternative scheme for filter bank based multicarrier transmission," in *Proc. Int. Symp. Commun. Control Signal Process. (ISCCSP)*, Roma, Italy, May 2–4 2012, pp. 1–4.

[9] D. Mattera, M. Tanda, and M. Bellanger, "Frequency-spreading implementation of OFDM/OQAM systems," in *Proc. Int. Symp. Wireless Commun. Syst. (ISWCS)*, Paris, France, Aug. 28–31 2012, pp. 176–180.

[10] M. Tanabe, A. Saito, M. Umehira, and S. Takeda, "A novel overlap FFT filter-bank using windowing and smoothing techniques to reduce adjacent channel interference for flexible spectrum access," in *Proc. Int. Conf. Inform. Commun. Technol. Convergence (ICTC)*, Jeju, South Korea, Oct. 19–21 2016, pp. 115–120.

[11] M. Renfors, J. Yli-Kaakinen, and f. harris, "Analysis and design of efficient and flexible fast-convolution based multirate filter banks," *IEEE Trans. Signal Processing*, vol. 62, no. 15, pp. 3768–3783, Aug. 2014.

[12] M. Renfors and J. Yli-Kaakinen, "Channel equalization in fast-convolution filter bank based receivers for professional mobile radio," in *Proc. European Wireless Conf. (EW)*, Barcelona, Spain, May 14–16 2014, pp. 844–848.

[13] J. Yli-Kaakinen and M. Renfors, "Multi-mode filter bank solution for broadband PMR coexistence with TETRA," in *Proc. 2014 European Conf. Networks and Commun. (EuCNC)*, Bologna, Italy, Jun. 23–24 2014, pp. 1–5.

[14] J. Bazzi, K. Kusume, P. Weitkemper, K. Takeda, and A. Benjebbour, "Transparent spectral confinement approach for 5G," in *Proc. European Conf. Networks and Commun. (EuCNC)*, Oulu, Finland, Jun. 12–15 2017, pp. 1–5.

[15] T. Levanen, J. Pirskanen, K. Pajukoski, M. Renfors, and M. Valkama, "Transparent Tx and Rx waveform processing for 5G new radio mobile communications," *IEEE Wireless Commun.*, vol. 26, no. 1, pp. 128–136, Feb. 2019.

[16] V. Vakilian, T. Wild, F. Schaich, S. ten Brink, and J. F. Frigon, "Universal-filtered multi-carrier technique for wireless systems beyond LTE," in *Proc. IEEE Globecom Workshops (GC Wkshps)*, Atlanta, GA, USA, Dec. 9–13 2013, pp. 223–228.

[17] X. Zhang, M. Jia, L. Chen, J. Ma, and J. Qiu, "Filtered-OFDM - Enabler for flexible waveform in the 5th generation cellular networks," in *Proc. IEEE Global Commun. Conf. (GLOBECOM)*, San Diego, CA, USA, Dec. 6–10 2015, pp. 1–6.

[18] J. Li, E. Bala, and R. Yang, "Resource block filtered-OFDM for future spectrally agile and power efficient systems," *Physical Communication*, vol. 11, pp. 36 – 55, 2014.

[19] R. Gerzaguet, D. Demmer, J. Doré, and D. Kténas, "Block-filtered OFDM: A new promising waveform for multi-service scenarios," in *Proc. IEEE Int. Conf. Commun. (ICC)*, Paris, France, May 22–23 2017, pp. 1–6.

[20] J. Nadal, C. A. Nour, and A. Baghdadi, "Novel UF-OFDM transmitter: Significant complexity reduction without signal approximation," *IEEE Trans. Veh. Technol.*, vol. 67, no. 3, pp. 2141–2154, Mar. 2018.

[21] M. Renfors, J. Yli-Kaakinen, T. Levanen, M. Valkama, T. Ihalainen, and J. Vihriala, "Efficient fast-convolution implementation of filtered CP-OFDM waveform processing for 5G," in *Proc. IEEE Globecom Workshops (GC Wkshps)*, San Diego, CA, USA, Dec. 6–10 2015, pp. 1–7.

[22] J. Yli-Kaakinen *et al.*, "Efficient fast-convolution-based waveform processing for 5G physical layer," *IEEE J. Select. Areas Commun.*, vol. 35, no. 6, pp. 1309–1326, Jun. 2017.

[23] H. V. Sorensen, C. S. Burrus, and D. L. Jones, "A new efficient algorithm for computing a few DFT points," in *Proc. IEEE Int. Symp. Circuits Syst. (ISCAS)*, vol. 2, Jun. 1988, pp. 1915–1918.

[24] H. V. Sorensen and C. S. Burrus, "Efficient computation of the DFT with only a subset of input or output points," *IEEE Trans. Signal Processing*, vol. 41, no. 3, pp. 1184–1200, Mar. 1993.

[25] R. E. Blahut, *Fast Algorithms and Multidimensional Convolutions*. Cambridge University Press, Jun. 2010.

[26] J. Cooley and J. Tukey, "An algorithm for the machine calculation of complex Fourier series," *Mathematics of Computation*, vol. 19, no. 90, pp. 297–301, 1965.

[27] M. Borgerding, "Turning overlap-save into a multiband mixing, downsampling filter bank," *IEEE Signal Processing Mag.*, vol. 23, no. 2, pp. 158–161, Mar. 2006.

[28] K. Shao, J. Alhava, J. Yli-Kaakinen, and M. Renfors, "Fast-convolution implementation of filter bank multicarrier waveform processing," in *Proc. IEEE Int. Symp. Circuits Syst. (ISCAS)*, Lisbon, Portugal, May 24–27 2015, pp. 978–981.

[29] H. Sorensen, M. Heideman, and C. Burrus, "On computing the split-radix FFT," *IEEE Trans. Acoust., Speech, Signal Processing*, vol. 34, no. 1, pp. 152–156, Feb. 1986.

[30] J. Yli-Kaakinen, P. Siohan, and M. Renfors, "FBMC design and implementation," in *Orthogonal Waveforms and Filter Banks for Future Communication Systems*, M. Renfors, X. Mestre, E. Kofidis, and F. Bader, Eds. Elsevier/Academic Press, 2017, ch. 8, pp. 157–195.

[31] J. Yli-Kaakinen and M. Renfors, "Optimized reconfigurable fast convolution based transmultiplexers for flexible radio access," *IEEE Trans. Circuits Syst. II*, vol. 65, no. 1, pp. 130–134, Jan. 2018.

[32] S.-C. Pei and T.-L. Luo, "Split-radix generalized fast Fourier transform," *Signal Processing*, vol. 54, no. 2, pp. 137 – 151, 1996.

[33] C. Boncelet, "A rearranged DFT algorithm requiring $N^2/6$ multiplications," *IEEE Trans. Acoust., Speech, Signal Processing*, vol. 34, no. 6, pp. 1658–1659, Dec. 1986.

[34] J. Yli-Kaakinen, T. Levanen, M. Renfors, M. Valkama, and K. Pajukoski, "FFT-domain signal processing for spectrally-enhanced CP-OFDM waveforms in 5G new radio," in *Proc. Asilomar Conf. Signals, Syst. Comput. (ACSSC)*, Pacific Grove, CA, USA, Oct. 28–31 2018.

[35] S. Mirabbasi and K. Martin, "Overlapped complex-modulated transmultiplexer filters with simplified design and superior stopbands," *IEEE Trans. Circuits Syst. II*, vol. 50, no. 8, pp. 456–469, Aug. 2003.

[36] L. G. Baltar, F. Schaich, M. Renfors, and J. A. Nossek, "Computational complexity analysis of advanced physical layers based on multicarrier modulation," in *Proc. Future Network Mobile Summit (FutureNetw), 2011*, Warsaw, Poland, Jun. 15–17 2011, pp. 1–8.

[37] D. Chen, D. Qu, T. Jiang, and Y. He, "Prototype filter optimization to minimize stopband energy with NPR constraint for filter bank multicarrier modulation systems," *IEEE Trans. Signal Processing*, vol. 61, no. 1, pp. 159–169, Jan. 2013.

[38] M. Abdelaziz, L. Anttila, M. Renfors, and M. Valkama, "PAPR reduction and digital predistortion for non-contiguous waveforms with well-localized spectrum," in *Proc. Int. Symp. Wireless Commun. Syst. (ISWCS)*, Poznan, Poland, Sep. 20–23 2016, pp. 581–585.

[39] 3GPP TR 38.900 V14.3.1, "Study on channel model for frequency spectrum above 6 GHz," Jul. 2017.

AlaaEddin Loulou received the Bachelor degree of electrical engineering from The Islamic University of Gaza, Palestine, in 2006 and the M.Sc. degree in information technology (with distinction) from Tampere University of Technology (TUT), Tampere, Finland, in 2013. He is currently pursuing the D.Sc.(Tech) degree in communication engineering in TUT.

Since 2012, he has held various research positions at TUT. His research interests are in enhanced OFDM waveforms and advanced multicarrier schemes.

Juha Yli-Kaakinen received the degree of Diploma Engineer in electrical engineering and Doctor of Technology (with honors) from Tampere University of Technology (TUT), Tampere, Finland, in 1998 and 2002, respectively.

Since 1995, he has held various research positions at TUT. His research interests are in digital signal processing, especially in digital filter and filter-bank optimization for communication systems and VLSI implementations.

Markku Renfors (S'77–M'82–SM'90–F'08) received the D.Tech. degree from Tampere University of Technology (TUT), Tampere, Finland, in 1982.

Since 1992, he has been a Professor with the Department of Electronics and Communications Engineering, TUT, where he was the Head from 1992 to 2010. His research interests include filter-bank based multicarrier systems and signal processing algorithms for flexible communications receivers and transmitters.

Dr. Renfors was a corecipient of the Guillemin Cauer Award (together with T. Saramäki) from the IEEE Circuits and Systems Society in 1987.